

Electronic Supplementary Information

**Restricted rotation and tunable fluorescence in atropisomeric naphthyl pyridine
chromophores**

Olga Yunyaeva,^a Duane Hean,^a Michael O. Wolf^{a*}

^aDepartment of Chemistry, University of British Columbia, 2036 Main Mall, Vancouver, British
Columbia, Canada V6T 1Z1

Table of Contents

Synthetic Schemes	2
Additional Figures	4
NMR Spectroscopy	9
Crystallography Data	23

Synthetic Schemes

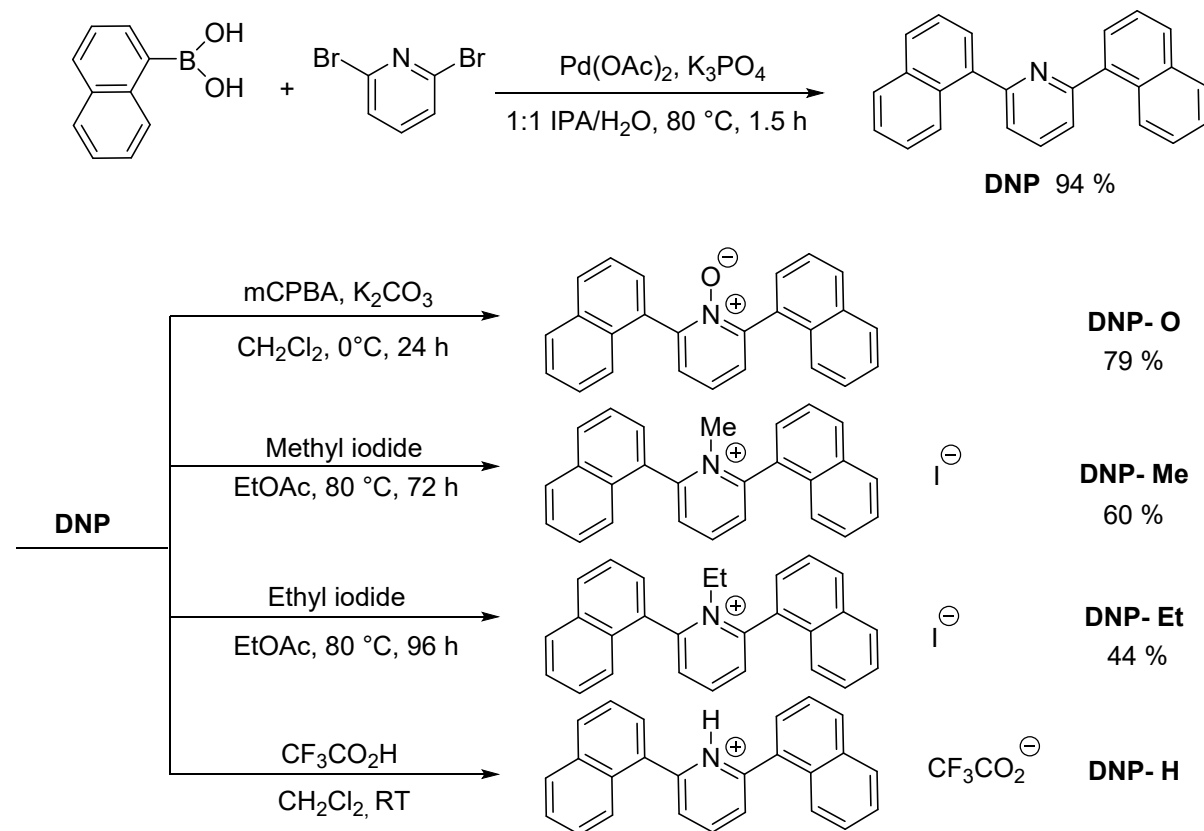


Figure S1. Synthetic route to disubstituted parent compound DNP and N-functionalized derivatives.

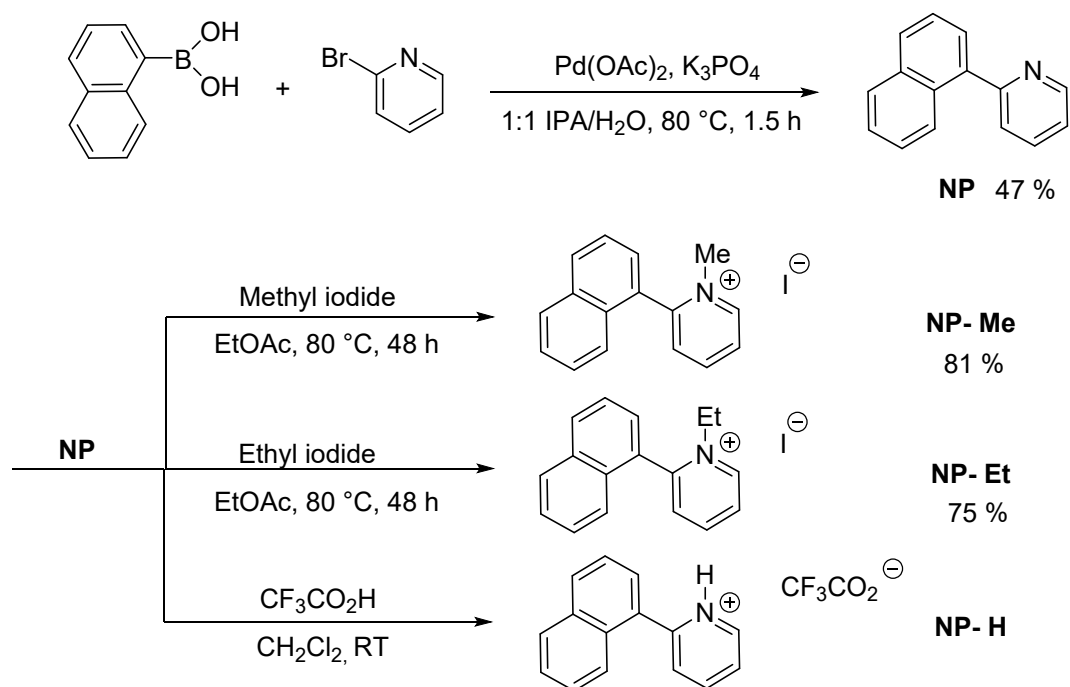


Figure S2. Synthetic route to monosubstituted parent compound NP and N-functionalized derivatives.

Additional Figures

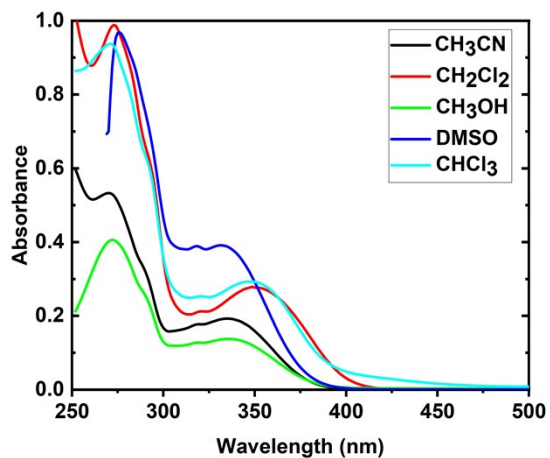


Figure S3. Absorption spectrum of **DNP-Me** in a range of solvents.

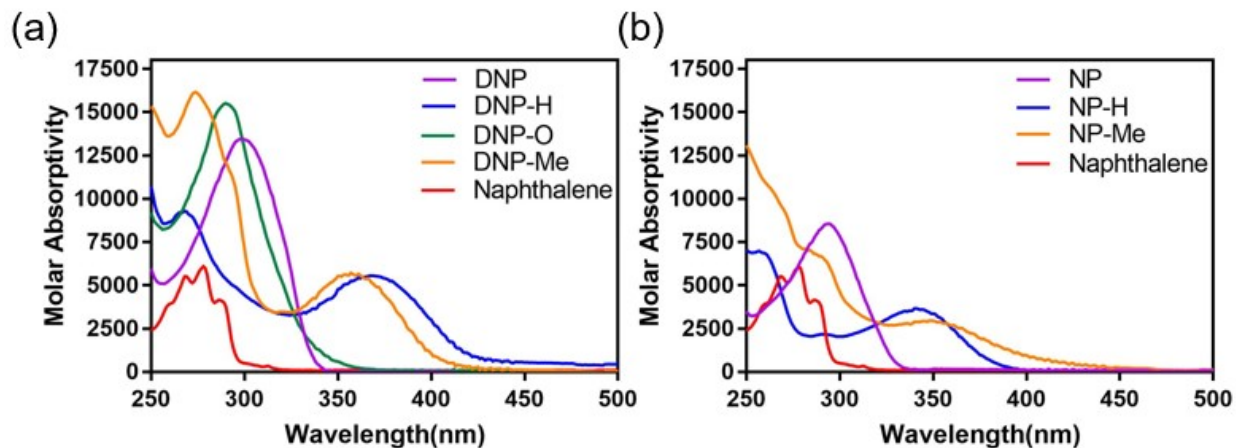


Figure S4. Molar absorptivity of (a) **DNP** and (b) **NP** compounds compared with naphthalene in CH_2Cl_2 .

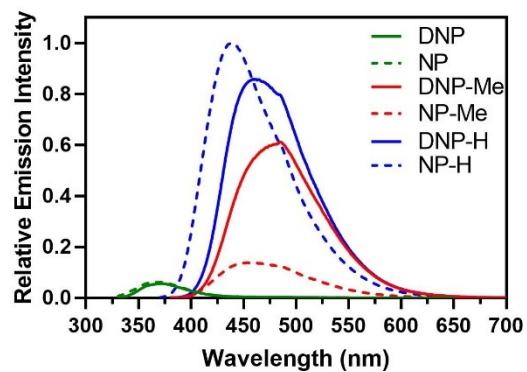


Figure S5. Relative emission spectra of **DNP** (solid line) and **NP** (dashed line) compounds taken in CH_2Cl_2 collected at an absorbance of 0.1, excited at λ_{max} .

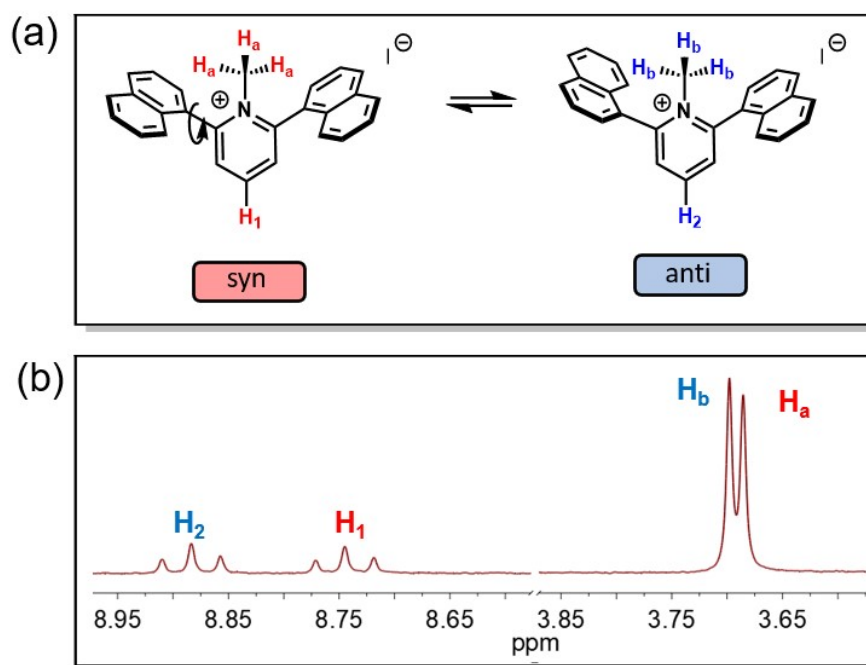


Figure S6. (a) Proposed conformations of two **DNP-Me** atropisomers (b) Portions of the ^1H NMR spectrum of **DNP-Me** in CD_2Cl_2 (400 MHz) at 25 °C.

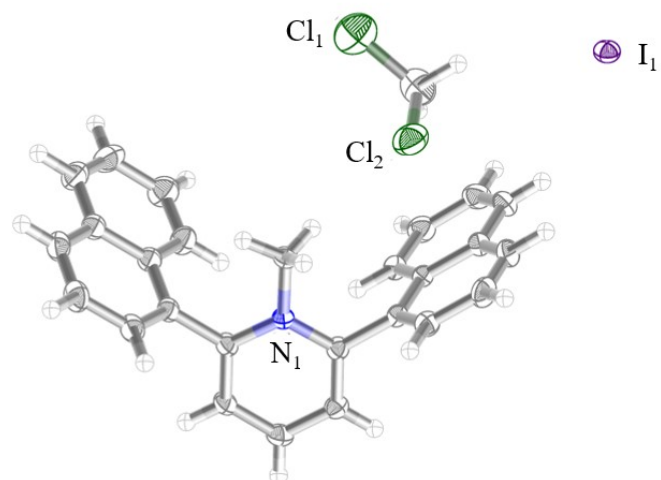


Figure S7. Crystal structure of **Me-DNP** with I⁻ as the counterion solvated with CH₂Cl₂.

Ellipsoids are plotted at the 50% probability level.

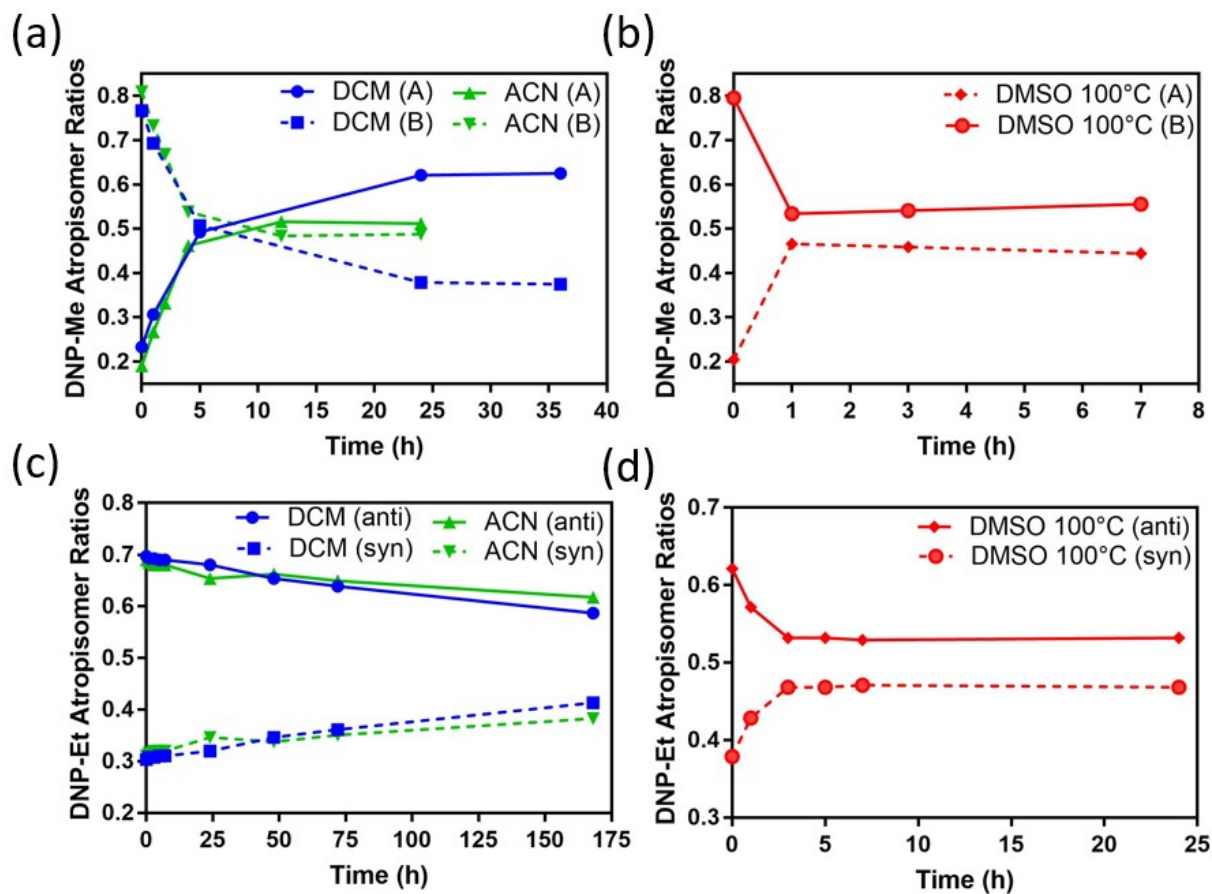


Figure S8. (a) Atropisomer ratios of **DNP-Me** over time in ambient light in CH_2Cl_2 and CH_3CN (b) and in DMSO at 100°C . (c) Atropisomer ratios of **DNP-Et** over time in ambient light in CH_2Cl_2 and CH_3CN (d) and in DMSO at 100°C .

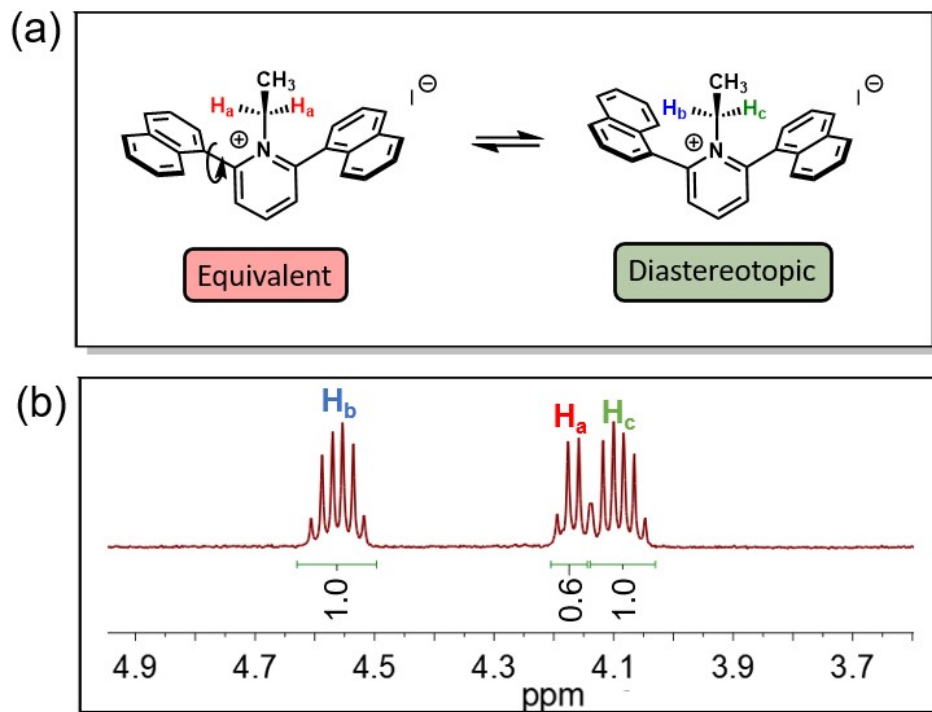


Figure S9. (a) Two atropisomers of **DNP-Et** and their conformations that lead to equivalent and diastereotopic peaks of the methylene protons in ^1H NMR. (b) Close up of the three methylene peaks present in the ^1H NMR spectrum of **DNP-Et** in CD_2Cl_2 (400 MHz at 25 °C) from δ 4.05-4.70, integrations relative to H_b and H_c , doublet of quartets.

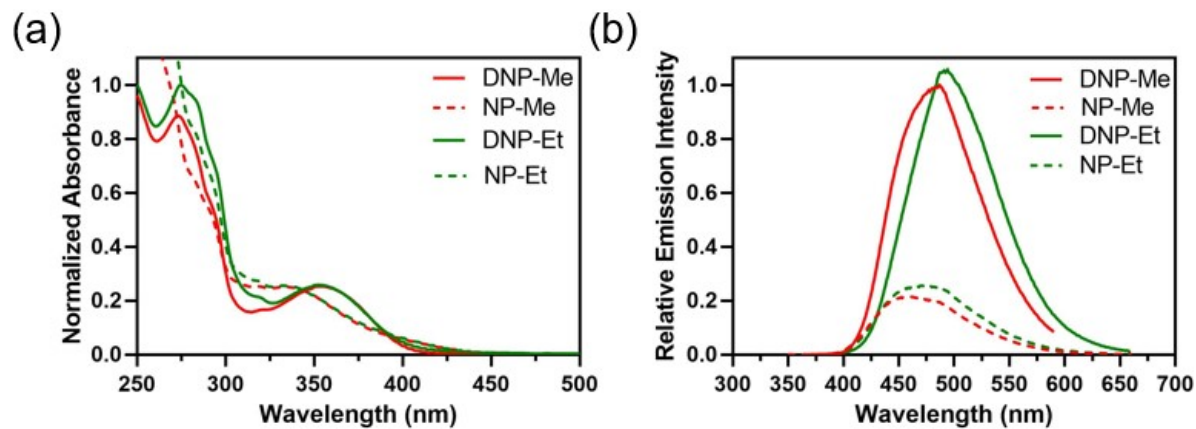


Figure S10. Relative (a) absorbance and (b) emission of **DNP-Me** and **DNP-Et** (solid line) and **NP** (dashed line) compounds in CH_2Cl_2 at 1×10^{-5} M collected at an absorbance of 0.1, excited at λ_{max} .

NMR Spectroscopy

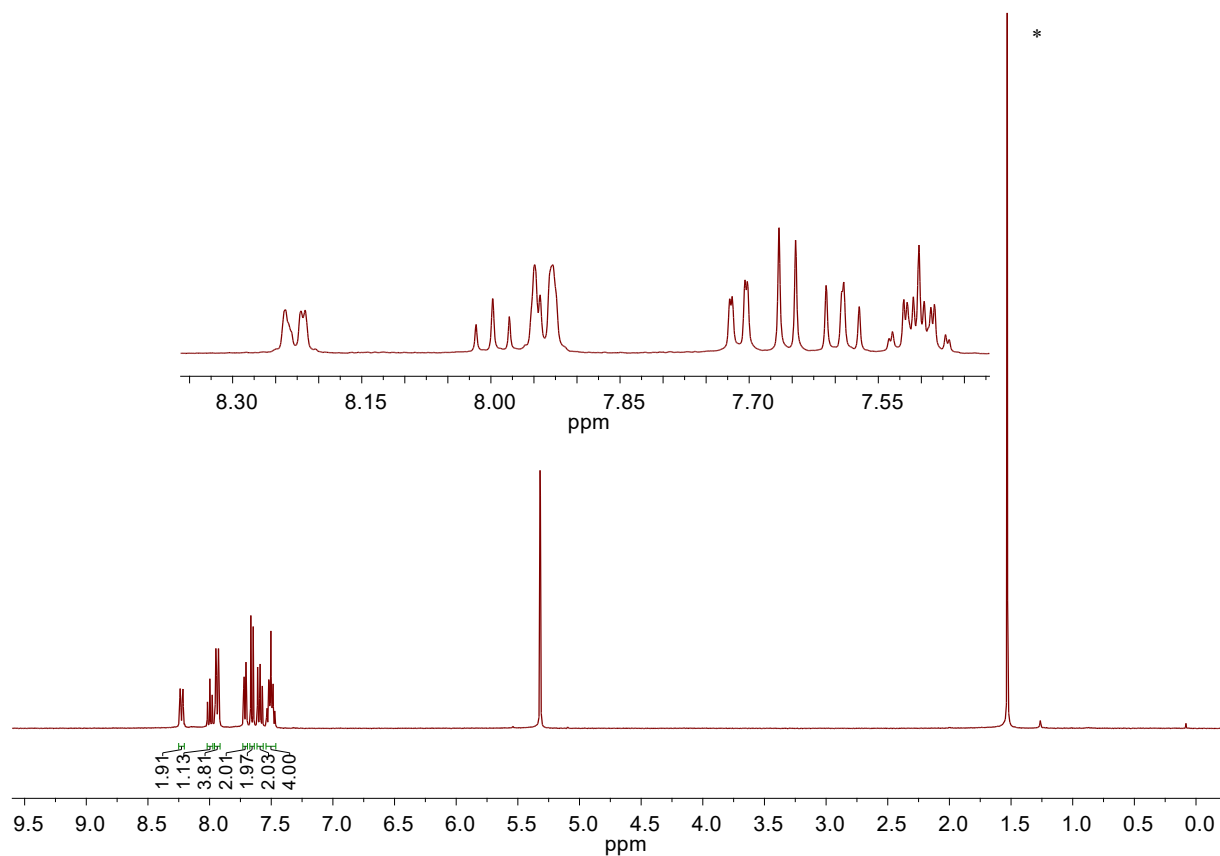


Figure S11. ^1H NMR spectrum of **DNP** (300 MHz, CD_2Cl_2) at 25°C . * = water.

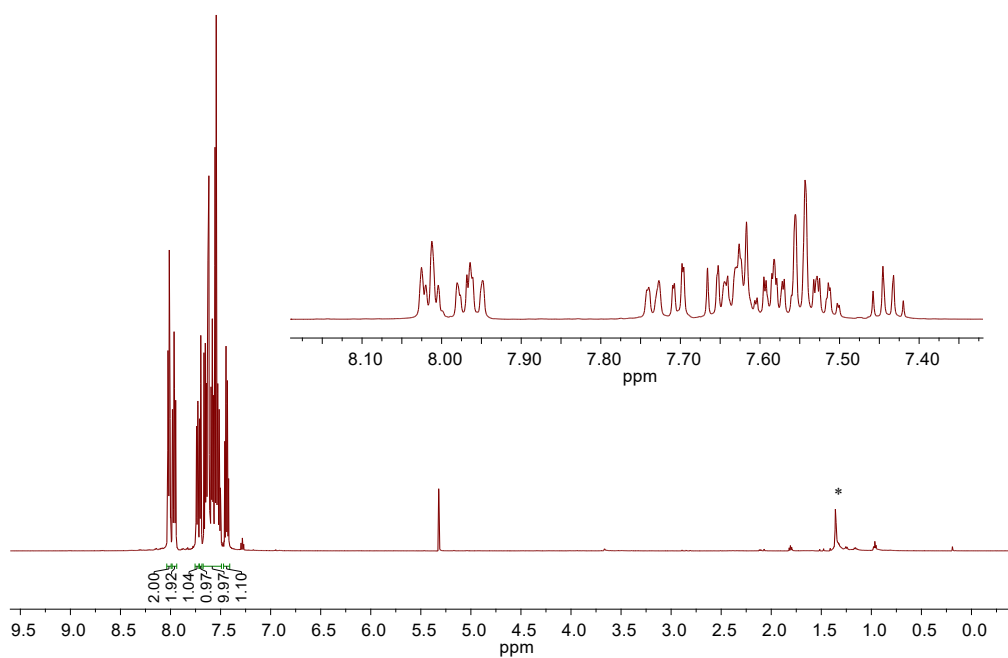


Figure S12. ¹H NMR spectrum of **DNP-O** (600 MHz, CD₂Cl₂) at 25°C, * = H grease

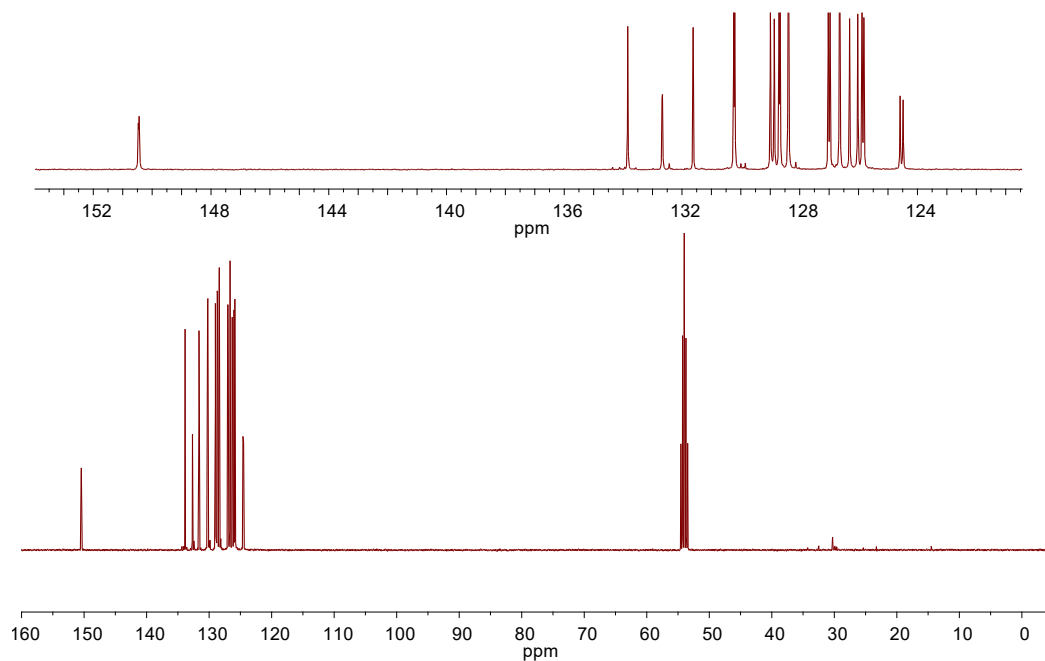


Figure S13. ¹³C NMR spectrum of **DNP-O** (101 MHz, CD₂Cl₂) at 25°C, peak doubling can be observed.

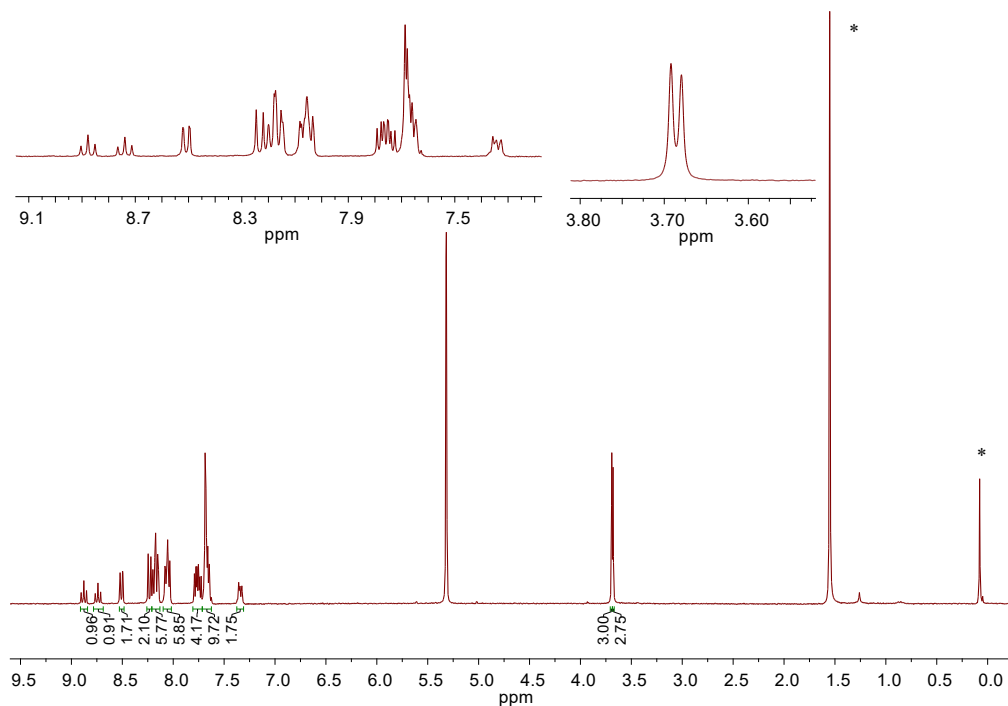


Figure S14. ^1H NMR spectrum of **DNP-Me** (300 MHz, CD_2Cl_2) at 25°C , doubling of the peaks can be seen.

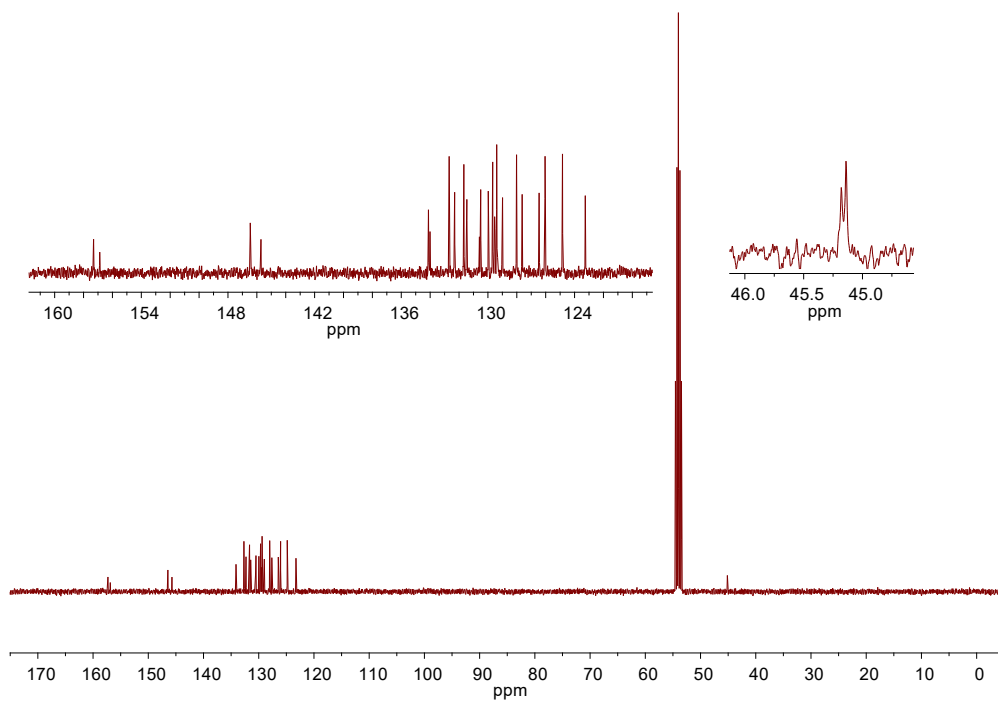


Figure S15. ^{13}C NMR spectrum of **DNP-Me** (101 MHz, CD_2Cl_2) at 25°C , doubling of the peaks can be seen.

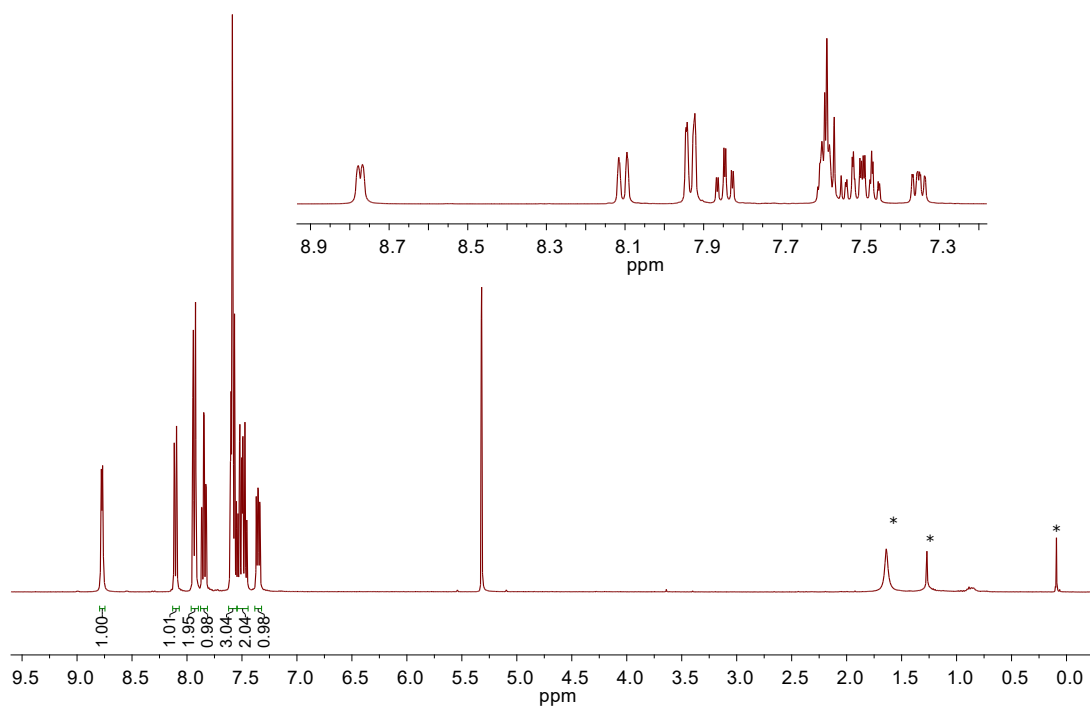


Figure S16. ^1H NMR spectrum of NP (300 MHz, CD_2Cl_2) at 25°C . * = water, hexanes, H grease.

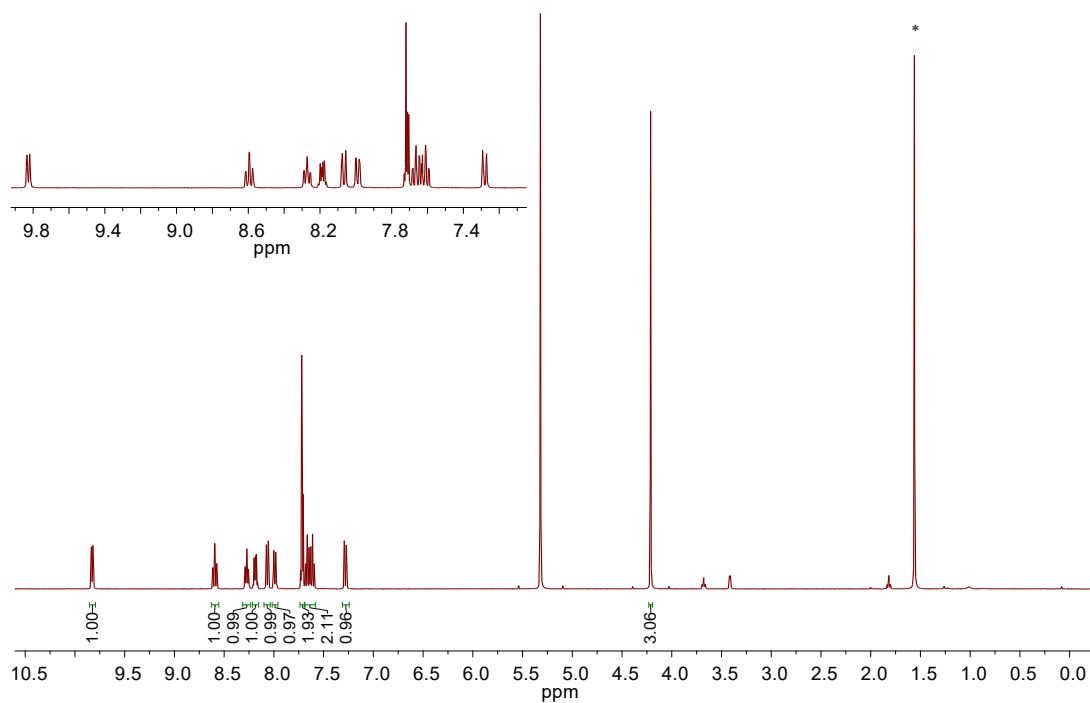


Figure S17. ^1H NMR spectrum of NP-Me (400 MHz, CD_2Cl_2) at 25°C . * = water.

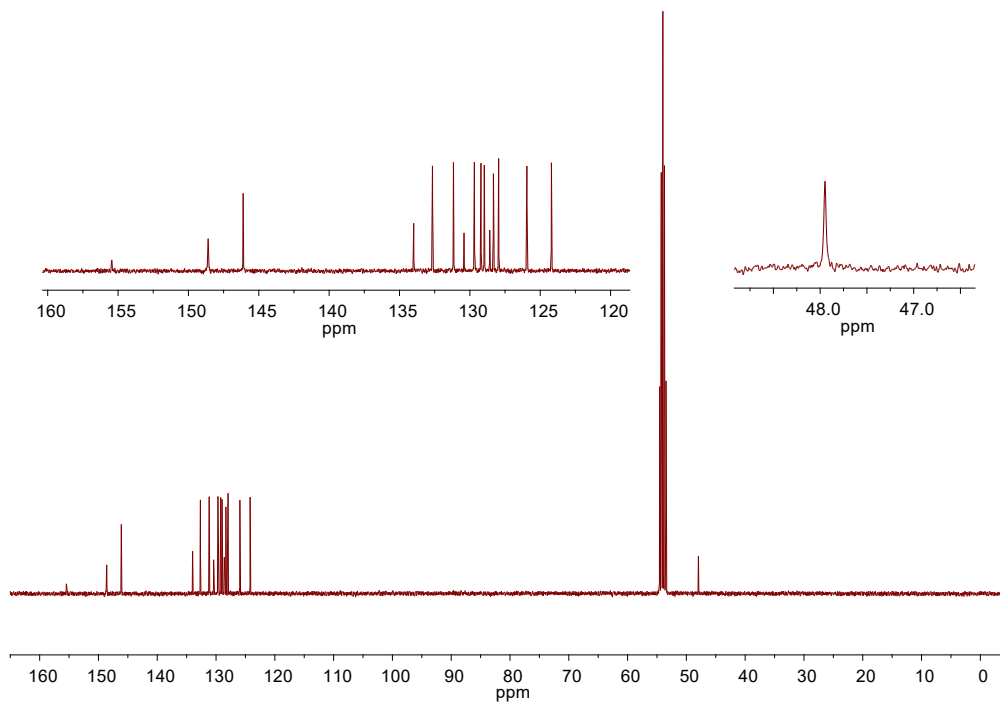


Figure S18. ^{13}C NMR spectrum of NP-Me (101 MHz, CD_2Cl_2) at 25°C .

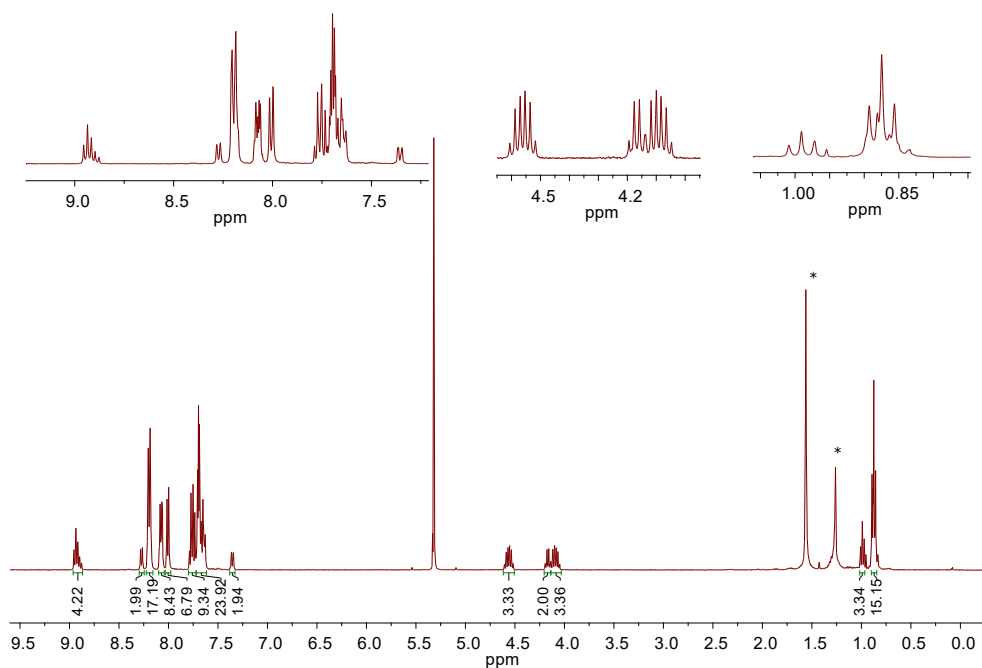


Figure S19. ^1H NMR spectrum of DNP-Et (400 MHz, CD_2Cl_2) at 25°C , doubling of the peaks can be seen, atropisomers are not in a 1:1 ratio, therefore integration does not accurately represent number of protons.

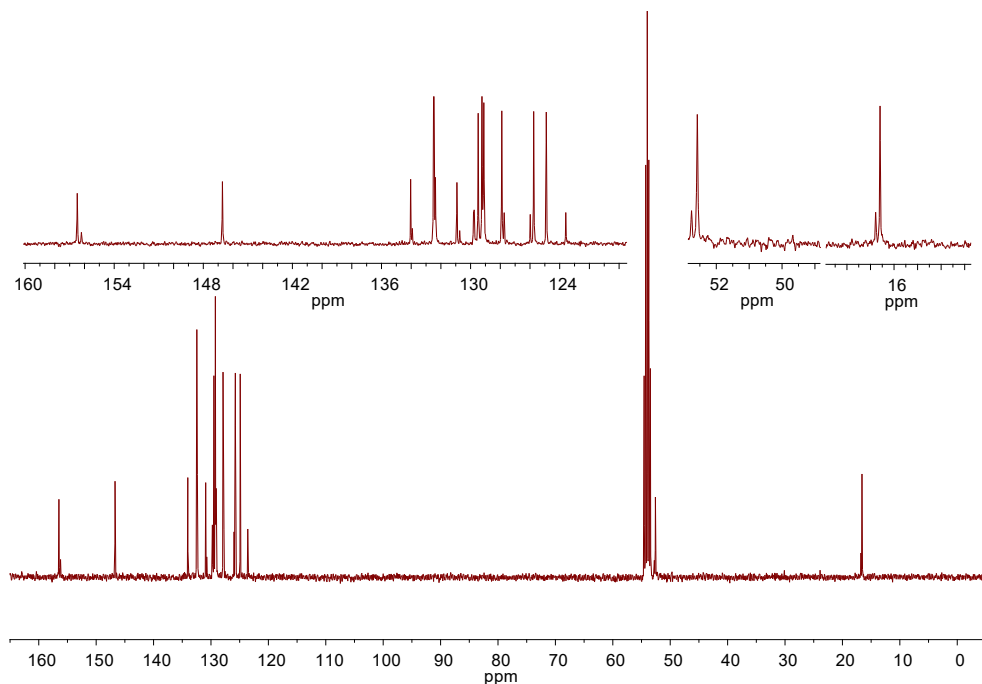


Figure S20. ^{13}C NMR spectrum of **DNP-Et** (101 MHz, CD_2Cl_2) at 25°C , doubling of the peaks can be seen.

* = water, H grease.

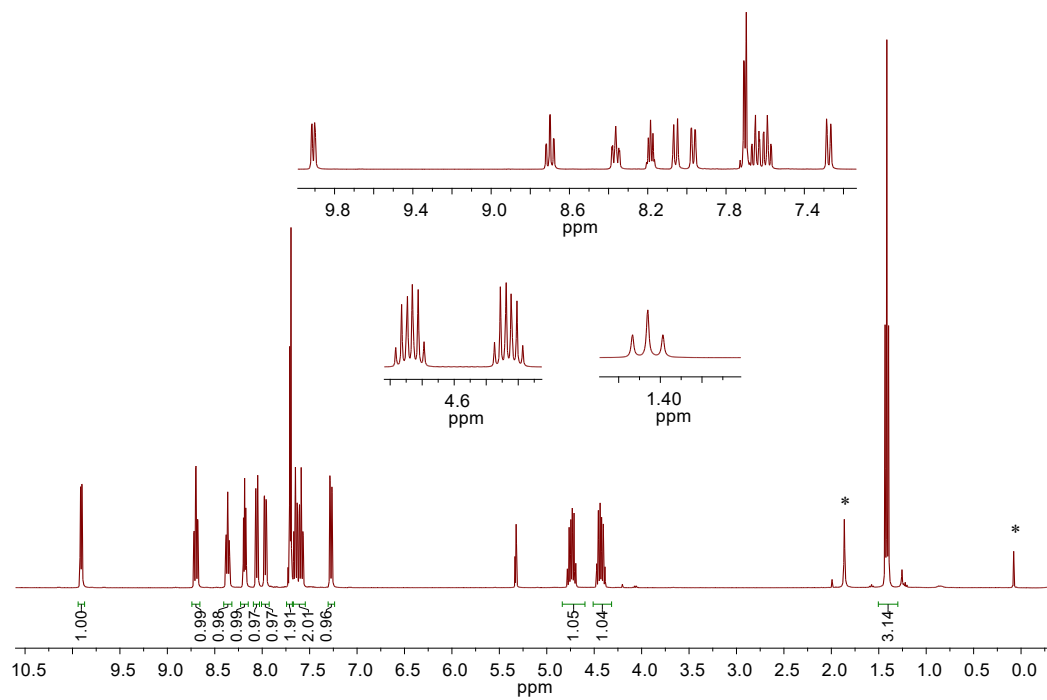


Figure S21. ^1H NMR spectrum of NP-Et (400 MHz, CD_2Cl_2) at 25°C .

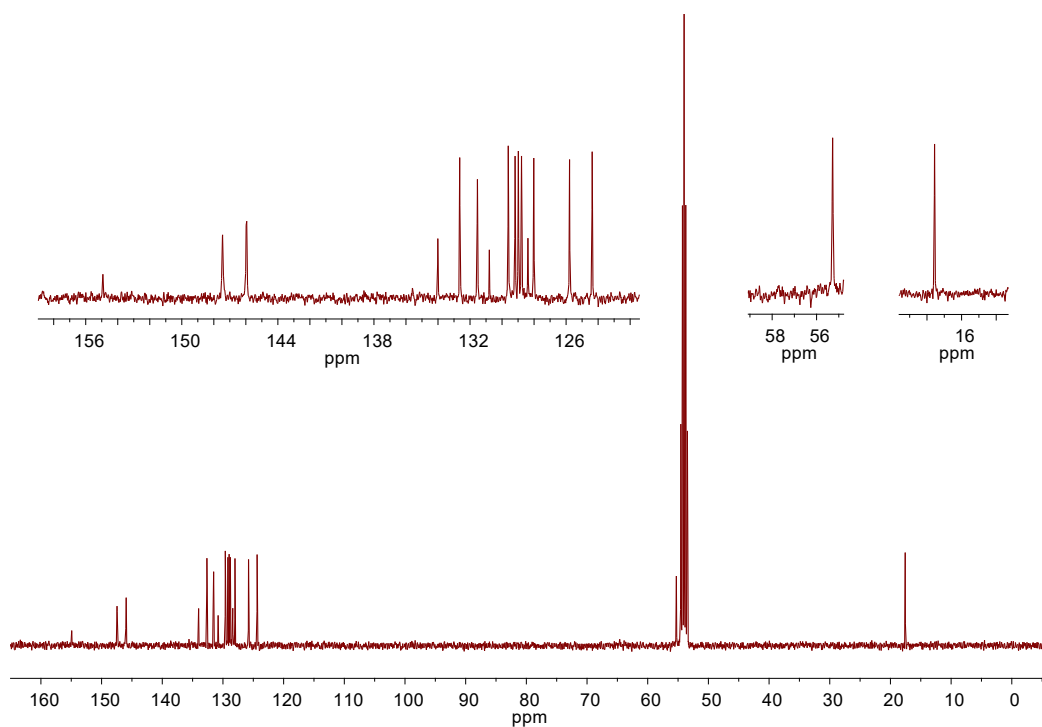


Figure S22. ^{13}C NMR spectrum of NP-Et (101 MHz, CD_2Cl_2) at 25°C .

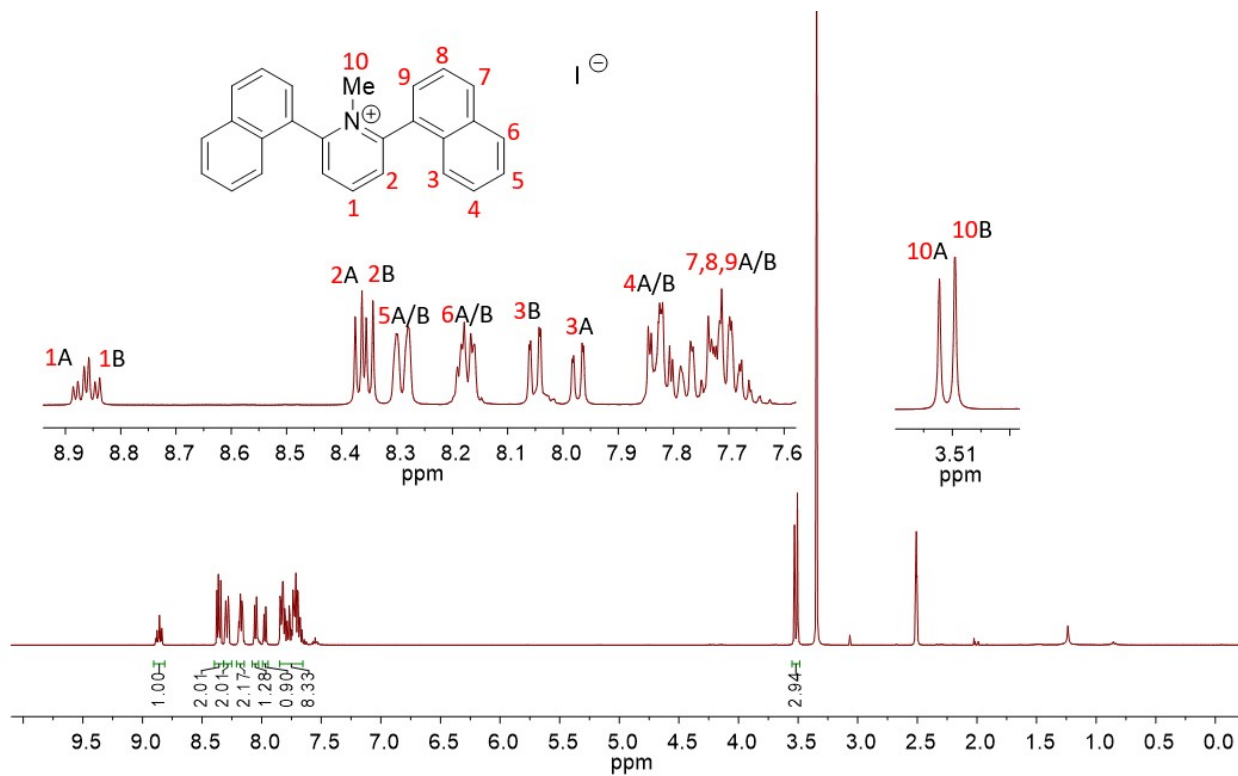


Figure S23. ¹H NMR spectrum of DNP-Me (400 MHz, DMSO-d₆) at 25°C. Atropisomer A/B is assigned.

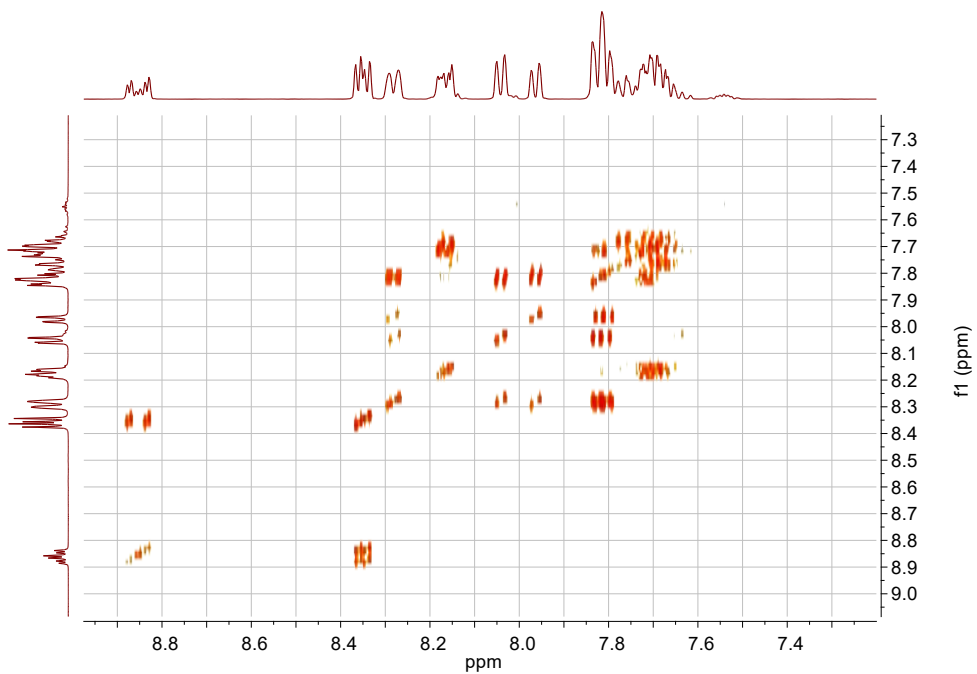
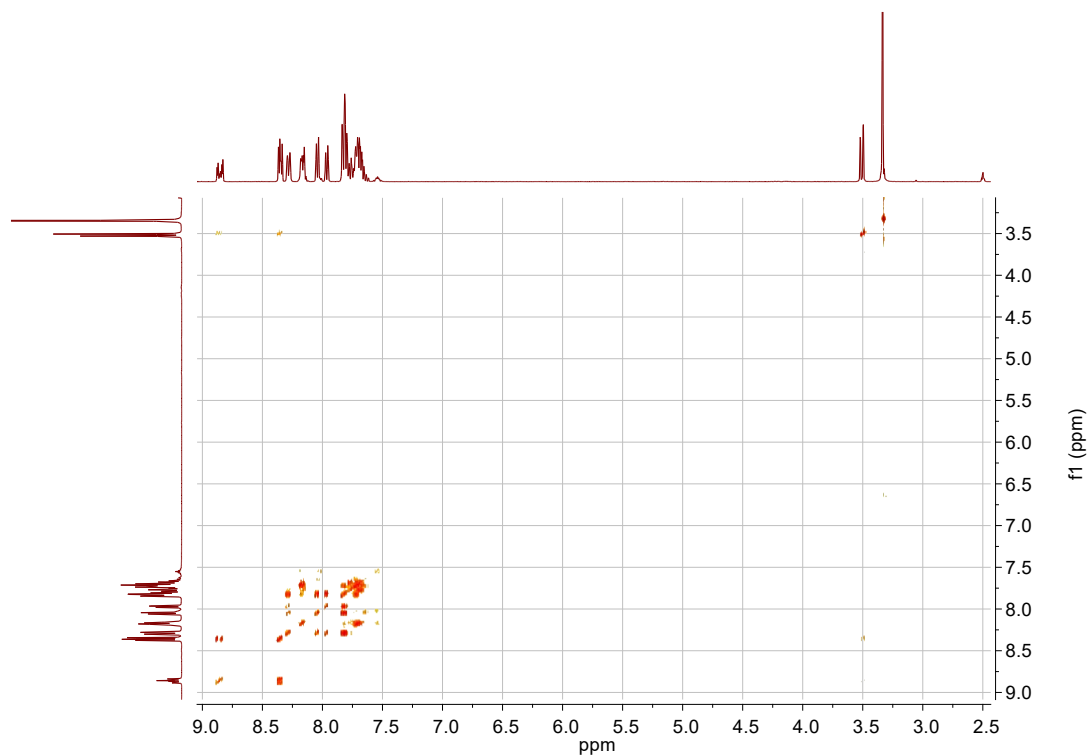


Figure S24. COSY spectrum of **DNP-Me** in DMSO-d_6 at 25°C .

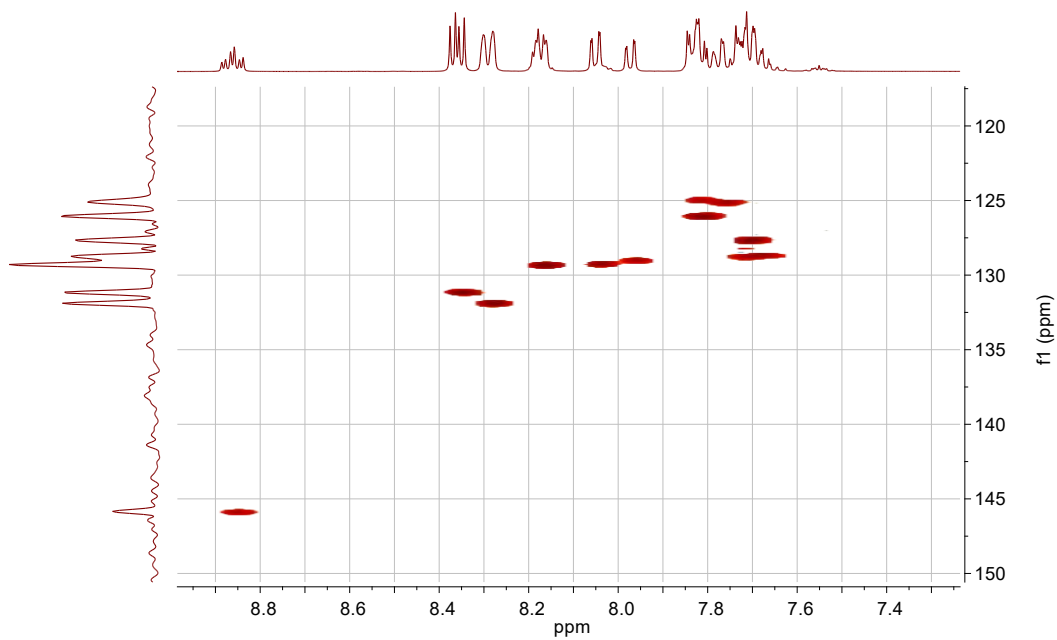
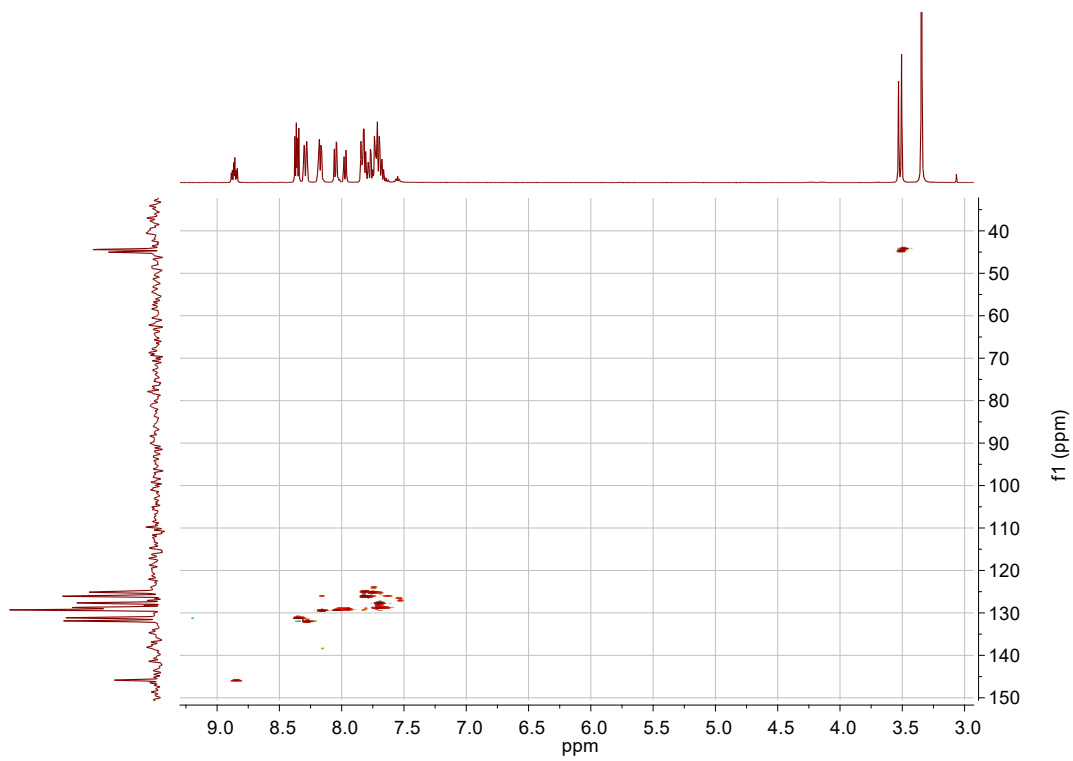


Figure S25. HSQC spectrum of **DNP-Me** in DMSO-d₆ at 25°C.

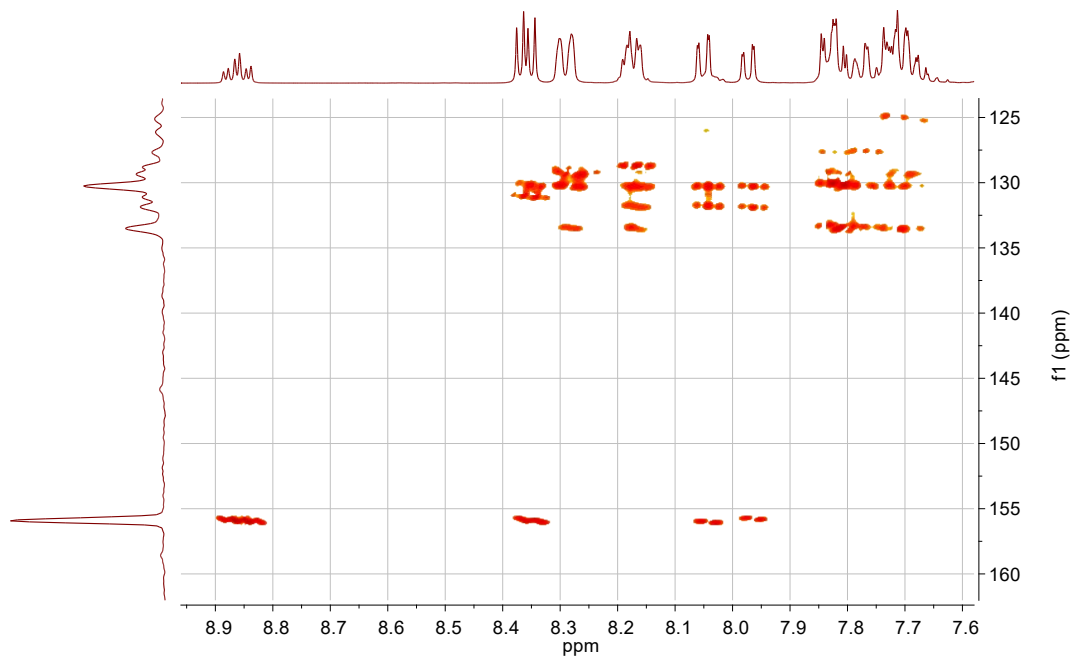
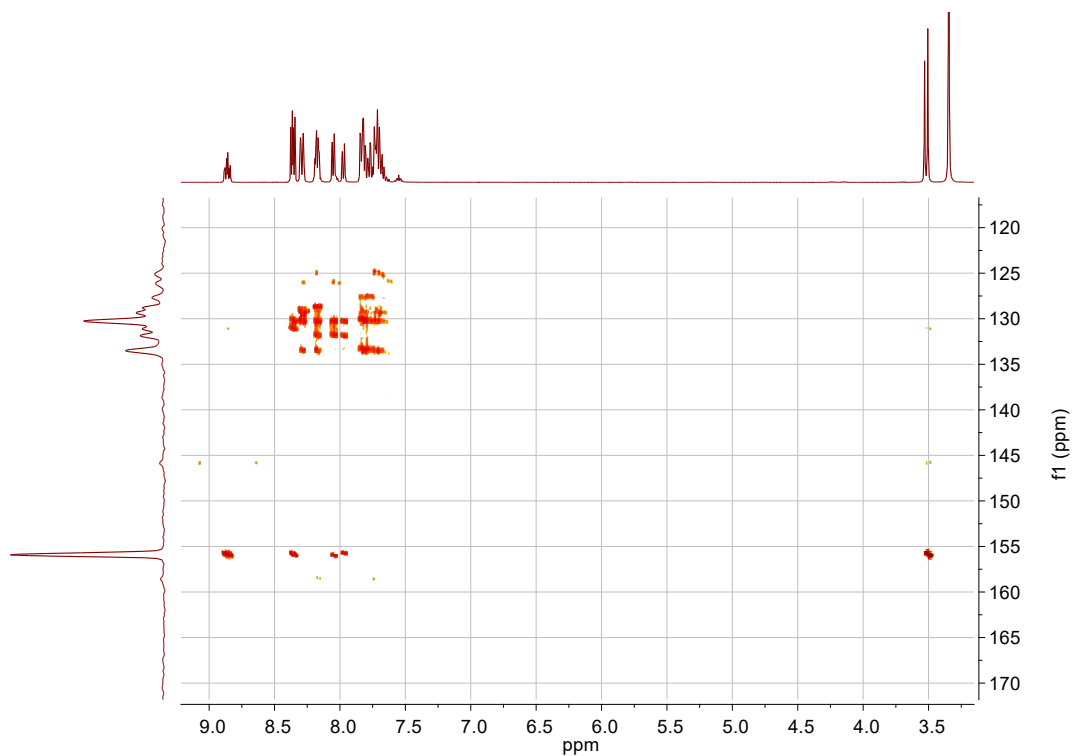


Figure S26. HMBC spectrum of **DNP-Me** in DMSO-d_6 at 25°C .

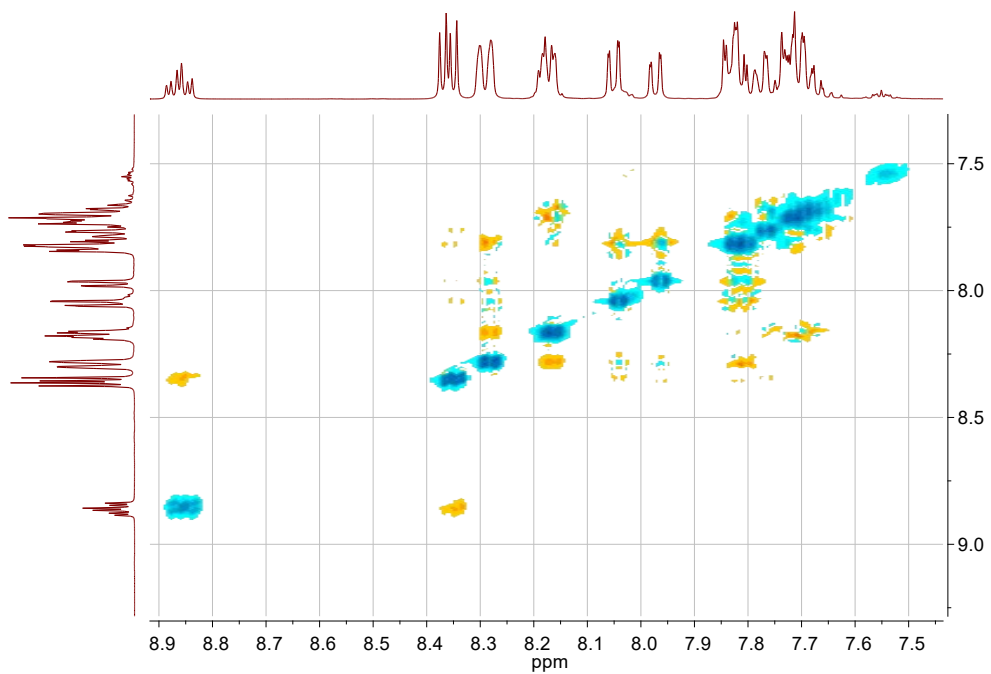
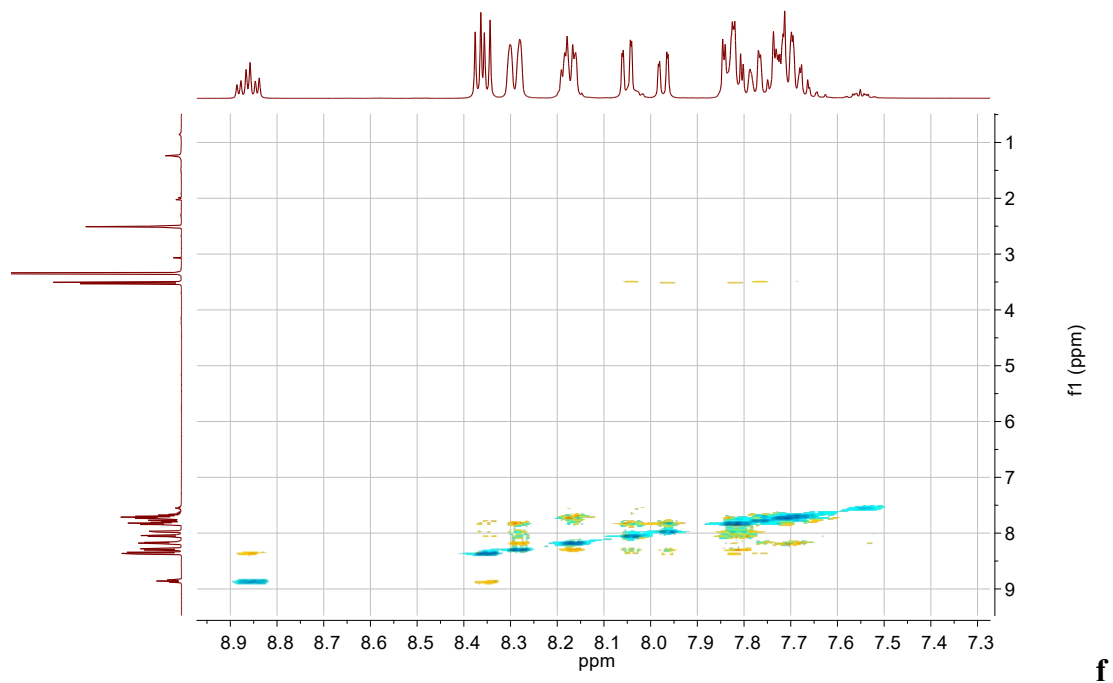


Figure S27. NOESY spectrum of **DNP-Me** in DMSO-d₆ at 25°C.

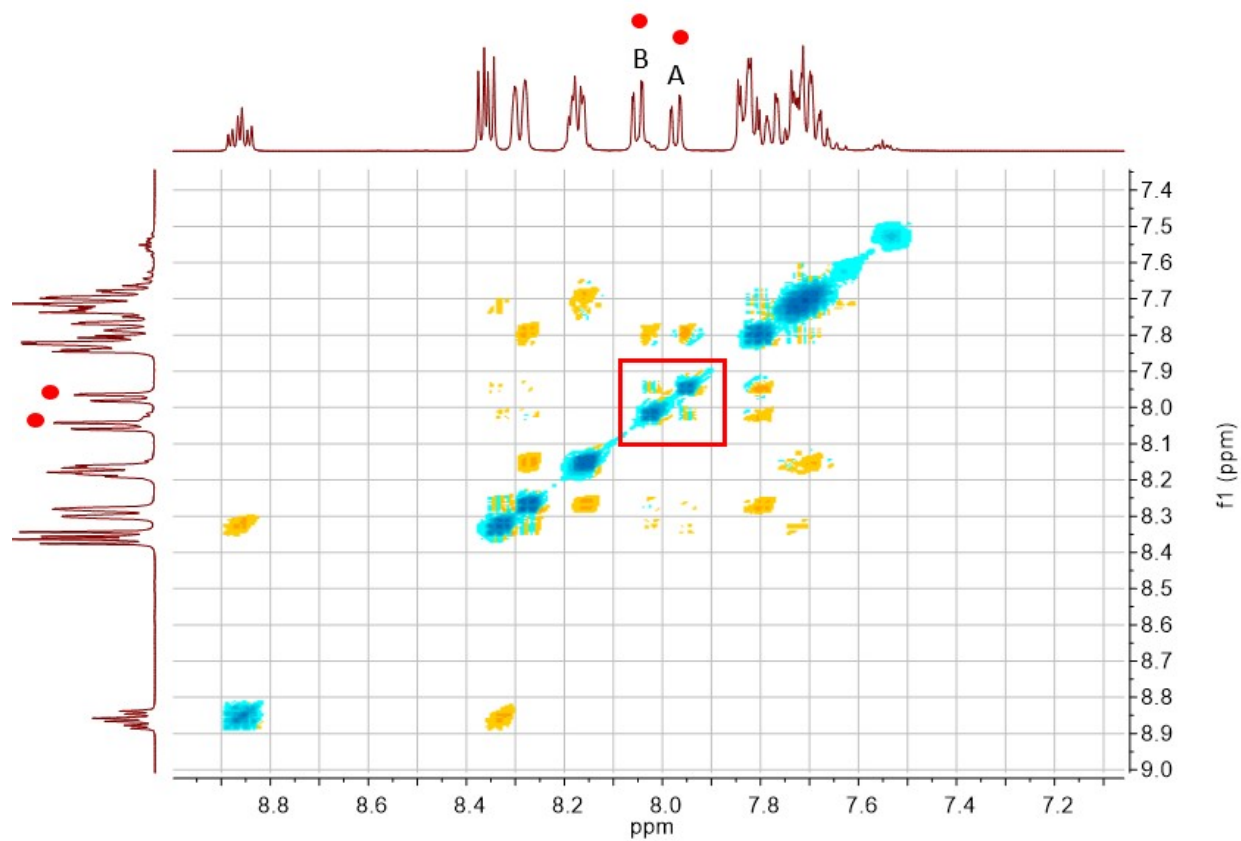


Figure S28. 2D NOESY spectra of **DNP-Me** in DMSO-d₆ at 75°C. Atropisomers A and B are distinguishable at $\delta = 8.05, 7.97$. A cross peak is present at elevated temperatures indicating chemical exchange is occurring between A and B.

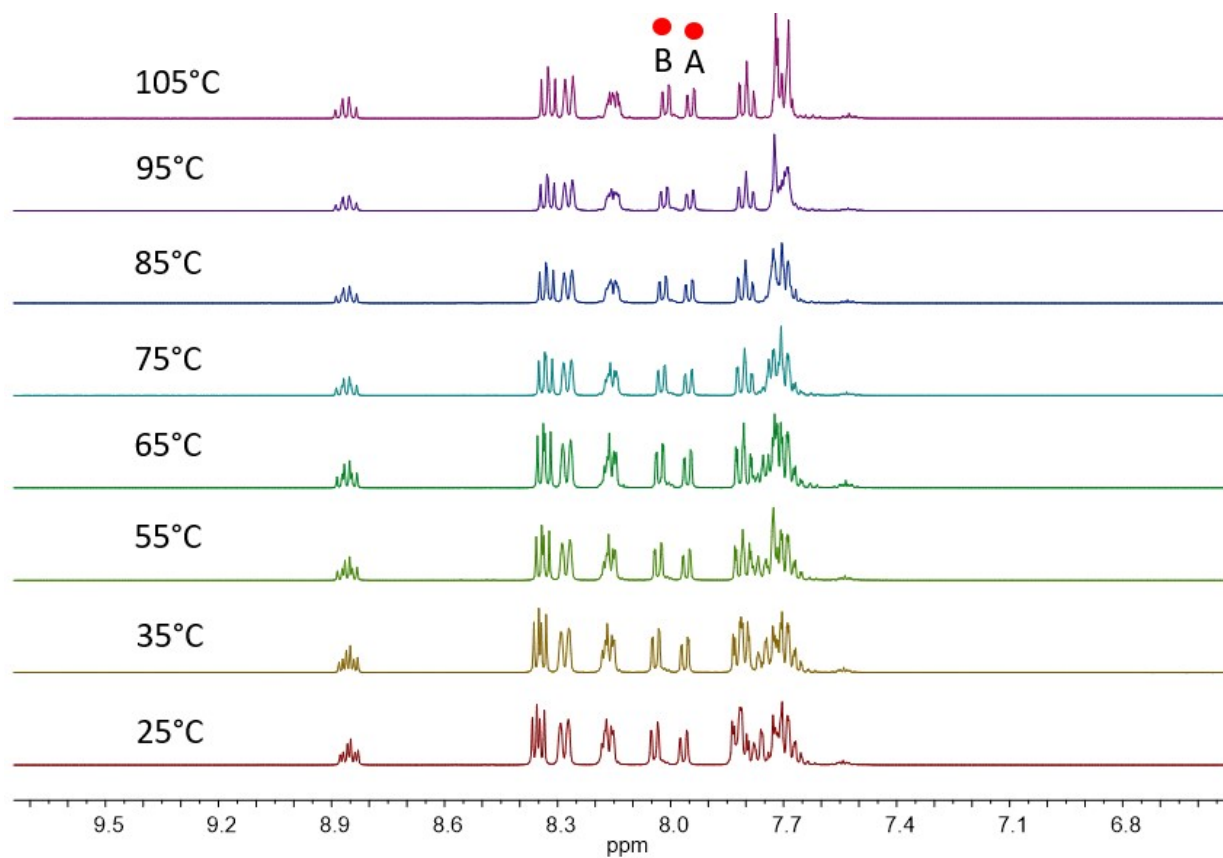


Figure S29. VT NMR of **DNP-Me** (400 MHz, DMSO-d₆) from 25-105 °C. The two red dots correspond to the two distinguishable protons of both DNP-Me atropisomers, no coalescence is seen and peaks stay separate and distinct from 25-105 °C.

Crystallography Data

Table S1. Crystal data and structure refinement for DNP-Me

Empirical formula	C ₂₇ H ₂₂ Cl ₂ IN
Formula weight	558.25
Temperature/K	296.15
Crystal system	Triclinic
Space group	P-1
a/Å	7.4594(5)
b/Å	11.1518(7)
c/Å	14.7331(9)
α/°	94.669(4)
β/°	101.035(4)
γ/°	99.434(4)
Volume/Å ³	1178.58(13)
Z	2
ρ _{calc} /g/cm ³	1.573
μ/mm ⁻¹	1.600
F(000)	556.0
Crystal size/mm ³	0.4 × 0.38 × 0.228
Radiation	MoKα (λ = 0.71073)
2θ range for data collection/°	2.836 to 61.154
Index ranges	-10 ≤ h ≤ 10, -15 ≤ k ≤ 15, -21 ≤ l ≤ 21
Reflections collected	25789
Independent reflections	7074 [R _{int} = 0.0349, R _{sigma} = 0.0351]
Data/restraints/parameters	7074/0/281
Goodness-of-fit on F ²	1.047
Final R indexes [I >= 2σ (I)]	R ₁ = 0.0381, wR ₂ = 0.0973
Final R indexes [all data]	R ₁ = 0.0439, wR ₂ = 0.1009
Largest diff. peak/hole / e Å ⁻³	1.72/-1.71